

UPDATE ON THE LOW EMITTANCE TUNING OF THE e^+/e^- FUTURE CIRCULAR COLLIDER

T. K. Charles^{*1}, Department of Physics, University of Liverpool, United Kingdom
B. Holzer, K. Oide², F. Zimmermann
European Organization for Nuclear Research (CERN), Geneva, Switzerland
¹also at The Cockcroft Institute, Daresbury, United Kingdom
²also at KEK, Oho, Tsukuba, Ibaraki, Japan

Abstract

The FCC-ee project studies the design of a future 100 km e^+/e^- circular collider for precision studies and rare decay observations in the range of 90 to 350 GeV center of mass energy with luminosities in the order of $10^{35} \text{ cm}^{-2} \text{ s}^{-1}$ [1,2]. To achieve ultra-low vertical emittance a highly effective emittance tuning scheme is required. In this paper, we describe a comprehensive correction strategy used for the low emittance tuning. The strategy includes Dispersion Free Steering, linear coupling compensation based on Resonant Driving Terms and beta beat correction utilising response matrices.

INTRODUCTION

FCC-ee project is a proposed 100 km circumference e^+/e^- collider that will operate at four beam energies: 45.6 GeV, 80 GeV, 120 GeV, and 182.5 GeV [1]. In this paper, we consider the 182.5 GeV 4IP ttbar lattice. Table 1 lists some of the key parameters. In order to reach the desired luminosity of $1.5 \times 10^{34} \text{ cm}^{-2} \text{ s}^{-1}$ at ttbar operation, low vertical emittance and strong focusing in the Interaction Region (IR) is required.

Table 1: Baseline Beam Parameters of the ttbar Operation of FCC-ee [1]

Parameters	$i\bar{i}$ lattice
Beam Energy [GeV]	182.5
Beam current [mA]	5.4
Number of bunches	33
ε_x [nm-rad]	1.45
ε_y [pm-rad]	2.7
β_x^* [mm]	1
β_y^* [mm]	1.6
\mathcal{L} [$10^{34} \text{ cm}^{-2} \text{ s}^{-1}$]	1.5

A comprehensive correction strategy is being developed to gradually reduce the vertical dispersion, beta beating, and coupling. This paper summarises some of the results of the present correction algorithm and strategy.

MISALIGNMENTS AND FIELD ERRORS

The size of the misalignments and field errors introduced, are listed in Table 2 and Table 3. These Tables show the

* tessa.charles@liverpool.ac.uk

rms value of the errors, that were introduced randomly via a Gaussian distribution truncated at 2.5 sigma. The definitions of the misalignments ΔX , ΔY , ΔPSI , and ΔS follow the MAD-X definitions, and are illustrated in Fig. 1.

The arc quadrupole and sextupoles were misaligned in MAD-X [3], and then through Python the girders were misaligned in x , y , and s , and rotated about the x and y axes. To introduce the girder rotations, two independent misalignments in both x and y were assigned to each end of the girder and the girder itself assumed rigid.

Table 2: RMS Magnet Misalignment Values (The definition of the Misalignment Parameters are Defined in Fig. 1)

Type	ΔX (μm)	ΔY (μm)	ΔPSI (μrad)	ΔS (μm)
Arc quadrupole*	50	50	400	150
Arc sextupoles*	50	50	400	150
Dipoles	1000	1000	400	1000
Girders	150	150	-	1000
IR quadrupole	100	100	250	250
IR sextupoles	100	100	250	250
BPM**	40	40	100	-

* misalignments relative to girder placement

** misalignments relative to quadrupole placement

Table 3: RMS Gradient Errors Used in All Simulations Presented in this Paper

Type	Field Errors
Arc quadrupole	$\Delta k/k = 2 \times 10^{-4}$
Arc sextupoles	$\Delta k/k = 2 \times 10^{-4}$
Dipoles	$\Delta B/B = 1 \times 10^{-4}$
IR quadrupole	$\Delta k/k = 2 \times 10^{-4}$
IR sextupoles	$\Delta k/k = 2 \times 10^{-4}$

GLOBAL CORRECTION ALGORITHM

Details of the correction algorithm can be found in previous publications [4–6]. In this paper, we share the results of the global correction strategy when applied to greater misalignments (than what was shown in earlier work), and we explore the influence of particular misalignment values, in a step towards defining alignment tolerances.

Content from this work may be used under the terms of the CC BY 3.0 licence (© 2021). Any distribution of this work must maintain attribution to the author(s), title of the work, publisher, and DOI

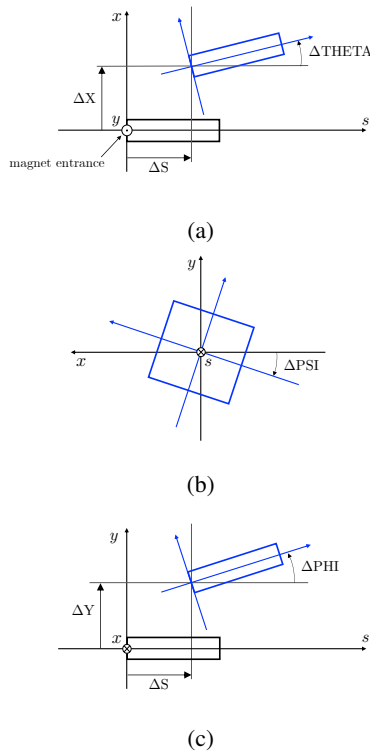


Figure 1: Definitions of misalignments errors, ΔX , ΔY , ΔPSI , and ΔS .

RESULTS

The correction algorithm was applied to 100 lattices with different random misalignments and gradient errors (i.e. using 100 random seeds) according to Table 2 and Table 1. Figure 2 shows the distributions of the emittances after correction, demonstrating that the small vertical emittance values can be achieved for a large number of seeds. The median of the distribution of horizontal emittances is 1.83 nm rad, which is noticeably larger than the design value of 1.45 nm rad that is achieved with an ideal lattice (i.e. perfect alignment and no field errors).

When the errors are first introduced, we set all the sextupole strengths to zero in order to find the closed orbit. Even with sextupoles off, we initially see a very large vertical dispersion around the ring, up to 2000 m in some locations. We then step through various orbit and optics corrections, gradually increasing the sextupole strength. Finally we arrive at well corrected vertical dispersion, with a final rms vertical dispersion of 0.495 mm being achieved.

The final beta beating for the same 100 seeds that were used to obtain Fig. 2, can be seen in Fig. 3. Most seeds show a final vertical beta beating of less than 5%.

Girder Misalignment

In order to determine the impact of specific misalignment types (in order to inform alignment tolerances), we set up a simulation campaign to study the effect of varying the various misalignment magnitudes one-by-one.

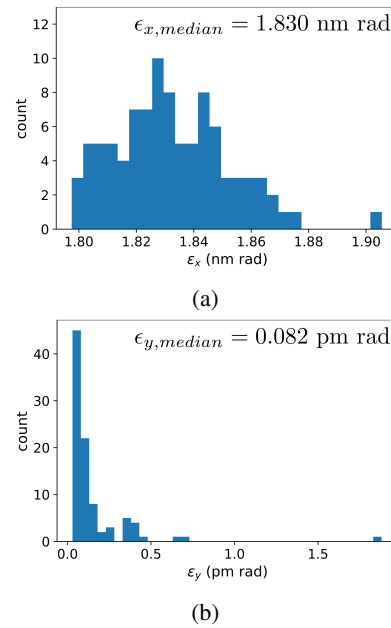


Figure 2: Distributions after global corrections of the a) horizontal emittance and b) vertical emittance for 100 lattices (i.e. 100 random seeds) with the field errors in Table 3 and the misalignments in Table 2.

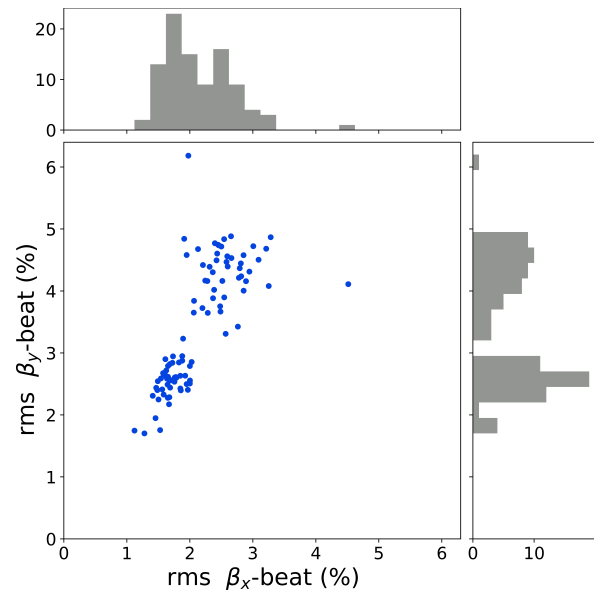


Figure 3: Beat beating after correction for 100 lattices (i.e. 100 random seeds) with the field errors in Table 3 and the misalignments in Table 2.

We varied the rms misalignment for girders whilst keeping all other errors the same as what is shown in Table 2 and Table 3. The results are shown in Fig. 4. There is a clear correlation between girder misalignment and the horizontal emittance growth. In fact, the girder misalignment has the strongest influence on horizontal emittance of all the parameters listed in Table 2. In the vertical plane, again the median emittance increases with girder misalignment,

but most noticeably the size of the errors also increase, indicating that we have a greater spread in the distributions of vertical emittances produced from different random seeds.

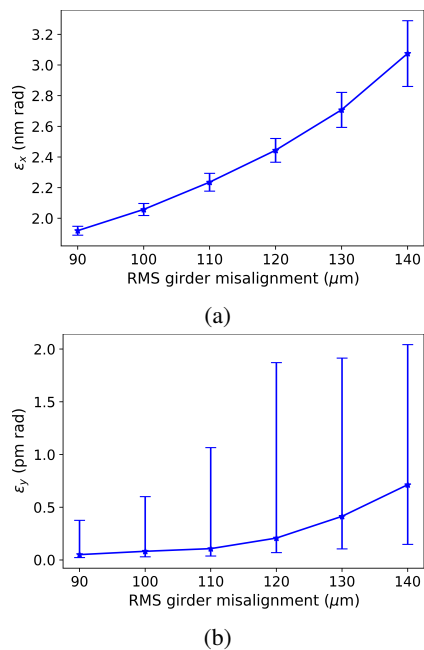


Figure 4: a) Median horizontal emittance and b) median vertical emittance variation with rms girder misalignment of ΔX and ΔY , after global corrections. Error bars show 90 % confidence interval. Misalignments of all magnets are specified in Table 2 and field errors in Table 3.

Arc Quads and Sextupole Misalignment

Similarly to the girder misalignment treatment, we considered the misalignment of the arc quadrupoles and sextupoles. In this case, all misalignment and field errors are as shown in Table 2 and Table 3, with the exception of girder misalignments, for this particular study which were: $\Delta X = 100 \mu\text{m}$ and $\Delta Y = 100 \mu\text{m}$.

Figure 5 shows the impact of increasing arc magnet misalignment on a girder. Two error bars indicate the 75% and 90% confidence intervals, revealing that as shown in Fig. 2, the majority of the seeds result in low emittance values, with a small number of seeds producing a tail to the histogram. These small number of seeds pull the 90% confidence interval bars further from the median.

Figure 6 shows the impact on the horizontal emittance, of increasing arc quadrupoles and sextupoles misalignment on a girder, whilst keeping the girder misalignments fixed at the four distinct levels of $\Delta X = \Delta Y = 80 \mu\text{m}$, $90 \mu\text{m}$, $100 \mu\text{m}$, and $110 \mu\text{m}$.

CONCLUSION

A comprehensive global correction strategy is being developed for FCC-ee. With an rms transverse girder misalignment tolerance of $150 \mu\text{m}$, and arc quadrupole and sextupole rms transverse misalignment tolerance of $50 \mu\text{m}$ (relative

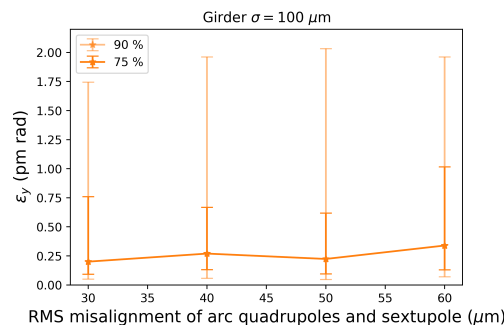


Figure 5: Median vertical emittance variation with rms misalignment of ΔX and ΔY of arc quadrupoles and sextupoles, for girder ΔX and ΔY misalignment of $100 \mu\text{m}$. The error bars show 75% (darker) and 90% (lighter) confidence intervals.

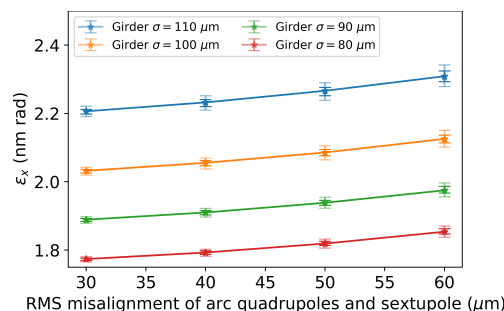


Figure 6: Median horizontal emittance variation with rms misalignment of ΔX and ΔY , of arc quadrupoles and sextupoles. Error bars show 75% (darker) and 90% (lighter) confidence intervals. Misalignments of all other magnets are specified in Table 2 and field errors, in Table 3.

to the girder), and the remaining magnets misaligned to reasonable values listed in the paper, the median vertical emittance after correction was found to be 0.082 pm rad and the median horizontal emittance was 1.83 nm rad . The vertical emittance is within the range of what is required and the horizontal emittance after correction, whilst larger than the ideal lattice, is still tolerable for the expected luminosity. This is an ongoing study to determine alignment tolerances required to reach the final emittance goal.

REFERENCES

- [1] A. Abada *et al.*, "FCC-ee: The lepton collider," *Eur. Phys. J. Spec. Top.*, vol. 228, pp. 261–623, 2019. doi:10.1140/epjst/e2019-900045-4
- [2] M. Mangano *et al.*, "FCC Physics Opportunities," *Eur. Phys. J. C*, vol. 79, p. 474, 2019. doi:10.1140/epjc/s10052-019-6904-3
- [3] MADX, <https://madx.web.cern.ch>
- [4] T. K. Charles, S. Aumon, B. Holzer, K. Oide, and F. Zimmermann, "Low emittance tuning of FCC-ee," *J. Phys. Conf. Ser.*, vol. 1350, p. 012006, 2019. doi:10.1140/epjst/e2019-900045-4
- [5] T. K. Charles, S. Aumon, B. J. Holzer, T. Tydecks, F. Zimmermann, and K. Oide, "Low-emittance Tuning for Circular Collid-

ers”, in *Proc. 62nd ICFA Advanced Beam Dynamics Workshop on High Luminosity Circular e+e- Colliders (eeFACT’18)*, Hong Kong, China, Sep. 2018, pp. 57.–62.
doi:10.18429/JACoW-eeFACT2018-TUOAB02

Proc. 10th Int. Particle Accelerator Conf. (IPAC’19), Melbourne, Australia, May 2019, pp. 574–577. doi:10.18429/JACoW-IPAC2019-MOPRB001

- [6] T. K. Charles, S. Aumon, B. J. Holzer, K. Oide, and F. Zimmermann, “Low Emittance Tuning of FCC-ee”, in